Accepted Manuscript

Title: Photocatalytic degradation and mineralization of perfluorooctanoic acid (PFOA) using a composite TiO_2 −rGO catalyst

Authors: Beatriz Gomez-Ruiz, Paula Ribao, Nazely Diban, Maria J. Rivero, Inmaculada Ortiz, Ane Urtiaga

PII: S0304-3894(17)30870-1
DOI: https://doi.org/10.1016/j.jhazmat.2017.11.048
Reference: HAZMAT 19019

To appear in: *Journal of Hazardous Materials*

Received date: 20-6-2017
Revised date: 24-11-2017
Accepted date: 25-11-2017

Please cite this article as: Beatriz Gomez-Ruiz, Paula Ribao, Nazely Diban, Maria J.Rivero, Inmaculada Ortiz, Ane Urtiaga, Photocatalytic degradation and mineralization of perfluorooctanoic acid (PFOA) using a composite TiO2 −rGO catalyst, Journal of Hazardous Materials https://doi.org/10.1016/j.jhazmat.2017.11.048

Photocatalytic degradation and mineralization of perfluorooctanoic acid (PFOA) using a composite TiO_2 -rGO catalyst

Authors:

Beatriz Gomez-Ruiz, Paula Ribao, Nazely Diban, Maria J. Rivero, Inmaculada Ortiz, Ane Urtiaga*

Department of Chemical and Biomolecular Engineering. Universidad de Cantabria. Av. de Los Castros s/n. 39005 Santander. Spain.

* Corresponding author: urtiaga@unican.es. Phone: +34 942201587

Submitted to

Journal of Hazardous Materials

November 2017

Graphical abstract

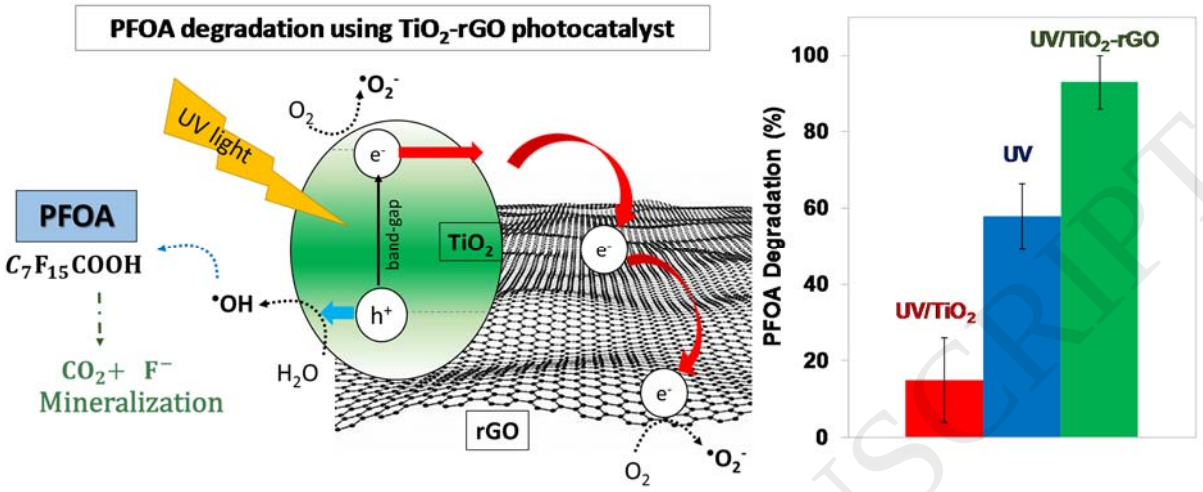

Highlights

- Photocatalytic decomposition of PFOA using a TiO_2-rGO catalyst was studied
- TiO_2-rGO catalyst (0.1 $g.L^{-1}$) allowed 93±7 % PFOA removal under UV-Vis irradiation
- Formation of intermediate PFCAs and F^- elucidated the PFOA degradation mechanism
- Faster degradation kinetics were observed for shorter carbon-chain PFCAs

ABSTRACT

The inherent resistance of perfluoroalkyl substances (PFASs) to biological degradation makes necessary to develop advanced technologies for the abatement of this group of hazardous substances. The present work investigated the photocatalytic decomposition of perfluorooctanoic acid (PFOA) using a composite catalyst based on TiO_2 and reduced graphene oxide (95% TiO_2/5% rGO) that was synthesized using a facile hydrothermal method. The efficient photoactivity of the TiO_2-rGO (0.1 $g.L^{-1}$) composite

was confirmed for PFOA (0.24 mmol.L^{-1}) degradation that reached 93±7% after 12 h of UV-visible irradiation using a medium pressure mercury lamp, a great improvement compared to the TiO_2 photocatalysis (24±11% PFOA removal) and direct photolysis (58±9%). These findings indicate that rGO provided the suited properties of TiO_2-rGO, possibly as a result of acting as electron acceptor and avoiding the high recombination electron/hole pairs. The release of fluoride and the formation of shorter-chain perfluorocarboxilyc acids, that were progressively eliminated in a good match with the analysed reduction of total organic carbon, is consistent with a step-by-step PFOA decomposition via photogenerated hydroxyl radicals. Finally, the apparent first order rate constants of the TiO_2-rGO UV-Vis PFOA decompositions, and the intermediate perfluorcarboxylic acids were found to increase as the length of the carbon chain was shorter.

Keywords: perfluorooctanoic acid, PFOA, TiO_2-rGO, Titanium dioxide, graphene oxide, photocatalysis

1. INTRODUCTION

The presence of poly- and perfluoroalkyl substances (PFASs) in industrial emissions, drinking water sources and groundwaters is of increasing concern due to their extreme persistence and potential toxicity [1–3]. As a result, the Stockholm Convention on Persistent Organic Pollutants restricted the use and production of perfluorooctanesulfonate (PFOS) and its salts, and at present perfluorooctanoic acid (PFOA) and PFOA related compounds are under review for listing under the Convention [4]. The United States Environmental Protection Agency established health advisory levels for PFOA and PFOS in drinking water at 0.07 $\mu g.L^{-1}$, both individually and combined [5].

Due to the inherent resistance of PFOA, PFOS and related compounds to biological degradation [6–8], there is an intense research on chemical oxidation/reduction technologies to degrade PFASs in water, including direct photolysis, photochemical oxidation, photochemical reduction, photocatalytic oxidation, electrochemical oxidation, persulfate oxidation and sonochemical pyrolysis [9–18]. Among these technologies, direct photolysis is an alternative that operates at ambient temperature and pressure and it does not require additional chemicals. However, the studies published so far have shown that PFOA was only efficiently decomposed using a light source emitting at wavelengths from deep UV-region to 220 nm [19,20] or under elevated irradiation intensity [21]. Therefore, direct photolysis application is constrained by the high energy demand needed to obtain the intensity of the active irradiating light and the long treatment times.

A literature survey about the photocatalytic PFOA degradation in aqueous media is summarized in Table S1 (Supplementary Material). Despite the suitable properties of

TiO_2 catalyst, such as non-toxicity, photostability and low cost [22–24], the majority of the previous studies revealed the low PFOA degradation rate achieved by TiO_2 photocatalysis, which was comprised in the range 7-44% in most of the studies [12,21,25–33]. The limited performance of TiO_2 is attributed to its relatively large band-gap, high recombination rate of electron-hole pairs and limited use of visible light spectrum. Nevertheless, the comparison of previous research is hindered by the diversity of the applied experimental conditions, e.g.: light intensity (0.45-9.5 $mW.cm^{-2}$), wavelength spectrum emitted by the light source (200-600 nm), reactor volume (0.12-3 L) and treatment time. The reaction medium has been also widely varied, in terms of PFOA concentration, background electrolytes and O_2 or N_2 supply [34]. Yet, the catalyst dosage was quite homogeneous in all the reviewed research, and was varied in the range of 0.25-2 $g.L^{-1}$. The highest reported PFOA removal rates, 98 %, could be associated to the use of high intensity irradiation, a factor that would accelerate the degradation rates [21,34].

Recently, different strategies have been proposed to overcome TiO_2 limitations, such as the synthesis of titanate nanotubes (TNTs) out of a commercial TiO_2 catalyst, that doubled the PFOA degradation rate [21]. Other approaches consisted of modifying the process conditions. Within this group, TiO_2-mediated photocatalysis combined with perchloric acid [26] or ultrasonication [35], achieved 2-fold and almost 5-fold improvements in the PFOA degradation rate, respectively. The addition of oxalic acid also accelerated PFOA decomposition using TiO_2, under nitrogen atmosphere [27]. However, these methods would involve adding different substances to the polluted water. A more promising strategy is focused on the synthesis of new composite catalysts that combine the photoactivity of TiO_2 with transition metals, e.g.: Fe, Nb, Cu, Pb [12,30,36] or with noble metal nanoparticles Ag, Pt or Pd [31]. Transition and noble

metals have demonstrated to act as electron traps preventing the high electron-hole recombination, to successfully improve the photocatalytic features of TiO_2-doped composites [37]. Also Song et al. [32] showed that the use of composites of TiO_2 with multiple wall carbon nanotubes (TiO_2-MWCNT) enhanced the photocatalytic PFOA decomposition.

Among the new strategies to enhance the efficiency of photocatalysts, the combination of TiO_2 with graphene materials has been reported to increase the lifetime of electron-hole pairs, by reducing charge recombination, due to the excellent electron trapping and electrical conductivity properties of graphene. It is also thought that graphene provides a superior photoresponse by extending the excitation wavelength compared to bare TiO_2 [37–40]. The effective photocatalytic activity of the composite catalysts based on TiO_2 and graphene or graphene oxide has been demonstrated for the degradation of dyes as model of organic pollutants [39,41–44], and in a few seminal studies dealing with more complex organic contaminants, such as, dodecylbenzenesulfonate [45], diphenhydramine [46] or phenols [40]. A notable gap is that TiO_2-graphene composite photocatalysts have not been tested yet for the degradation of neither PFOA nor other PFASs.

This study aims to explore the photocatalytic degradation of PFOA by means of a composite catalyst of TiO_2 and reduced graphene oxide (TiO_2-rGO). Photocatalysis experiments under UV-visible irradiation examined the effect of TiO_2-rGO catalyst concentration on PFOA removal and defluorination, and evaluated the generation of shorter-chain perfluorinated intermediate products, as well as the total organic carbon reduction. Results were compared with bare TiO_2 and direct photolysis conditions to gain insight into factors influencing the significant photocatalytic enhancement that was

provided by the TiO_2-rGO material. Finally, this work assessed the effect of the alkyl chain length on the kinetics of the photocatalytic degradation of perfluorocarboxylic acids by means of TiO_2-rGO composite catalyst.

2. MATERIALS AND METHODS

2.1.Chemical Reagents

All chemicals were reagent grade or higher and were used as received without further purification. PFOA ($C_7F_{15}COOH$, 96% purity), perfluoroheptanoic acid (PFHpA, $C_6F_{13}COOH$, 99% purity), perfluorohexanoic acid (PFHxA, $C_5F_{11}COOH$, 96% purity), perfluoropentanoic acid (PFPeA, C_4F_9COOH, 97% purity) were purchased from Sigma Aldrich Chemicals. TiO_2 (P25, 20% rutile and 80% anatase, 50 $m^2.g^{-1}$, 21 nm) was obtained from Evonik Degussa. Graphite powder was supplied by Acros Organics. Sulfuric Acid 95-98% (H_2SO_4), chloride acid 37% (HCl), potassium permanganate ($KMnO_4$), sodium nitrate ($NaNO_3$), phosphoric acid (85%) and sodium di-hydrogen phosphate anhydrous were provided by Panreac. Hydrogen peroxide (H_2O_2, 30% v/v) and Methanol (UHPLC-MS grade) were obtained from Scharlau. All solutions were prepared using ultrapure water (Q-POD Millipore).

2.2.Synthesis of composite TiO_2-rGO catalyst.

The first step was the synthesis of graphene oxide (GO) using the modified Hummers method [47] by the oxidation of graphite powder with $NaNO_3$, H_2SO_4 and $KMnO_4$. The oxidized graphite was centrifuged and washed with ultrapure water and with an aqueous HCl solution. The remaining solid was ultrasonicated to achieve exfoliated graphene oxide nanosheets. After that, the sample was centrifuged and the supernatant was collected and dried in an oven overnight, obtaining GO as a solid [46].

TiO_2-rGO composites were synthesized using the hydrothermal method and following the procedure reported in the literature [37,48]. In brief, commercial TiO_2 was added into 150 mL GO dispersion in ultrapure water. The content of GO was controlled to be 5% wt. in the TiO_2-rGO composites. After stirring for 2 h, the solution was placed in a 200 mL Teflon-lined stainless steel auto-clave and maintained at 120 ºC for 3 h, to achieve simultaneously the reduction of GO and the loading of TiO_2 on the reduced GO sheets. The resulting composite was recovered by centrifugation, rinsed with ultrapure water, and fully dried at 50 ºC overnight.

The successful synthesis of the composite TiO_2-rGO was examined by means of Attenuated Total Reflectance Fourier Transformed Infrared (ATR-FTIR) spectroscopy (Fig. S1, Supplementary Material). The intensity increase of the ATR-FTIR bands between 500-900 cm-1 for TiO_2-rGO in contrast to the TiO_2 material was indicating the formation of Ti-O-C bonds in addition to the typical Ti-O-Ti bonds present in TiO_2. Furthermore, Transmission Electron Microscopy (TEM) results (Fig. S2 in supplementary material) demonstrated the homogeneous distribution of the TiO_2 catalysts on the rGO surface. Energy dispersive X-ray (EDX) spectroscopy of two distinct zones of the TiO_2-rGO material were done to qualitatively discern between TiO_2 and GO presence. Both ATR-FTIR and TEM-EDX results are similar to those reported by Ribao et al [37]. X-ray diffraction analysis (Fig. S3 in supplementary material) showed that the crystalline phase of the commercial P25 TiO_2 was maintained in the TiO_2-rGO composite after the hydrothermal sysnthesis. Therefore, it can be deemed that TiO_2-rGO composites were successfully prepared via hydrothermal synthesis. Finally, the specific surface area (*S*) of the catalyst materials was calculated by the Brunauer-Emmett-Teller (BET) method from the nitrogen adsorption-desorption isotherm data employing the ASAP 2000 surface area analyzer (Micromeritics).

2.3.Photocatalytic experiments

The schematic of experimental setup is shown in the Supplementary Material, Fig. S4. Photocatalytic experiments were conducted in a 1 L Heraeus Laboratory UV Reactor mounted on an Agimatic-S magnetic stirring plate (JP Selecta, Spain). A water/ethylene-glycol cooling jacket (PolyScience Digital Temperature Controller) was used to keep the reactor temperature at 293-298 K. A medium-pressure mercury lamp (Heraus Noblelight TQ 150 W z1) with an emission spectrum between 200 and 600 nm (Fig. S5, supplementary material) was used as irradiation source. The lamp was placed in a quartz sleeve in the centre of the reactor. It is noteworthy that the quart sleeve of the lamp did not absorb light in the UV wavelength range of interest. PFOA aqueous solutions 0.24 mmol.L^{-1} were used as feed in all experiments. The initial pH of the PFOA solution was 3.8 and it was not adjusted during the experiments. The TiO_2-rGO catalyst doses were 0.05, 0.1 and 0.5 g.L^{-1}. Samples were withdrawn from the reactor at different time intervals and filtered through 0.45 µm polypropylene filters to remove the catalyst particles before analysis. A HD2102.1 photo/radiometer (Delta OHM) provided with VIS-NIR, UVA, UVB and UVC detectors allowed measuring the light intensity received on the outer wall of the glass reactor.

2.4.Analytical methods

The concentration of PFOA and its degradation products, PFHpA, PFHxA, PFPeA were analysed using HPLC-DAD (Water 2695) system equipped with a X Bridge C18 column (5 µm, 250 mm x 4.6 mm, Waters). The separation column was set in an oven at 40 ºC. A mixture of methanol (65%) and di-hydrogen phosphate (35%) was used as mobile phase in isocratic mode with a flow rate of 0.5 mL.min^{-1}. The wavelength of the detector was set at 204 nm. The limit of quantification (LOQ) was 10 mg.L^{-1} for PFOA

and 5 mg.L^{-1} for PFHpA, PFHxA and PFPeA.

TOC analyses were performed using a TOC-V CPH (Shimadzu). Fluoride was analyzed by ion chromatography (Dionex 120 IC) provided with an IonPac As-HC column and using a 9 mM Na_2CO_3 solution as eluent, that was circulated at a flowrate of 1 mL.min^{-1}, based on Standard Methods 4110B (Standard Methods, 1998). The LOQ for fluoride analysis was 0.03 mg.L^{-1}. The possible fluoride incorporation onto the TiO_2-rGO surface was investigated by X-ray photoelectron spectroscopy (XPS), using an SPECS (Berlin, Germany) system equipped with a Phoibos 150 1D-DLD analyser and monochromatic Al K_α radiation (1486.6 eV).

3. RESULTS AND DISCUSSION

3.1.Photocatalytic decomposition of PFOA

The photocatalytic degradation of PFOA using the TiO_2-rGO composite and commercial TiO_2 was studied. Moreover, the removal of PFOA by direct photolysis under UV irradiation was also studied for comparison. The intermediate products formed upon PFOA degradation were analysed, and PFOA mineralization rate was monitored using the progress of TOC and the released fluoride as indicators. The adsorption of PFOA in the experimental system was negligible (less than 1%) after 12 h of contact of the feed solution inside the glass reactor. The amount of PFOA adsorbed on the TiO_2 and TiO_2-rGO (0.5 g.L^{-1}) were found to be 6.4±0.6% and 8.4±0.4%, respectively, after 12 h of contact under stirring in dark conditions. These values of adsorption could be explained by the higher BET specific surface area of TiO_2-rGO, $S_{TiO2\text{-}rGO}$ = 62.2 $m^2.g^{-1}$, compared to TiO_2, S_{TiO2}=50 $m^2.g^{-1}$ [48]. Similar values of PFOA adsorption on TiO_2 and metal-modified TiO_2 have been reported [31]. The electrostatic attraction between the negatively charged perfluorooctanoate anion and the positively

charged surface of TiO_2 particles in acidic solution could have favoured the adsorption [12,26], that nevertheless reached only a minor fraction of the initial content.

Next, the influence of the photocatalytic media was assessed. Fig. 1 allows the comparison of the disappearance of PFOA with time by means of direct photolysis (without catalyst) and when using TiO_2 and TiO_2-rGO as photocatalysts. In every experiment, a volume of 0.8 L of an aqueous PFOA solution (0.24 $mmol.L^{-1}$) was irradiated. It is observed that the application of UV light in the absence of any catalyst produced a significant PFOA degradation that reached 58 ± 9% removal after 12 h of irradiation. These results are in agreement with available data reported elsewhere [9,21]. PFOA molecule strongly absorbs light with wavelengths from deep UV-region to 220 nm, and presents weak absorption in the 220-270 nm range of light wavelengths [19]. In line with these properties, some authors reported high PFOA photoabatement using a vacuum UV lamp with a monochromatic emission at 185 nm, although the kinetics of PFOA removal were significantly reduced when using the more common emission at 254 nm [49,50]. However, the comparison of literature data about the direct photolysis of PFOA is hindered by the diversity of the applied experimental conditions, range of UV emission wavelength and power of the UV lamp [21]. In line with the previous discussion, it was concluded that the medium-pressure mercury lamp used in the present study promoted PFOA degradation by means of the deep UV-region of its emission spectrum.

The addition of the TiO_2 catalyst (Fig. 1, UV-TiO_2) had the effect of decreasing the PFOA removal to only 24 ± 11%, after 12 h of irradiation. Although PFOA could have been partially adsorbed on the TiO_2 surface (6.4% adsorption was observed in the dark experiments), the little release of fluoride (0.14 $mmol.L^{-1}$) and the detection of a small

amount of PFHpA (0.023 mmol.L^{-1}) confirmed that PFOA had been partially degraded into shorter-chain perflurocarboxylic acids. The lower degradation rate of PFOA observed upon the addition of TiO_2 can be assigned to a light screening effect by the TiO_2 particles, that would have significantly reduced the penetration of the UV light into the reaction medium [51]. In contrast, the use of the TiO_2-rGO composite (Fig. 1, UV-TiO_2-rGO) enhanced PFOA degradation compared to direct photolysis and TiO_2-mediated photocatalysis. 93 ± 7% of the initial PFOA was removed after 12 h of irradiation, 4-fold higher than in TiO_2-mediated photocatalysis for the same reaction time. This high degradation has been previously demonstrated in the literature using TiO_2 catalysts modified with metals such as Pb [36]. Moreover, a control experiment using GO nanoplatelets showed that graphene oxide particles did not produce a significant variation of PFOA concentration, at the same time no degradation products were detected in solution. This result pointed out a synergistic effect between the reduced graphene oxide (rGO) layers and TiO_2 nanoparticles during the photocatalytic degradation of PFOA. The effect can be ascribed to the good transparency of one-atom thickness rGO sheets towards the UV-visible spectrum, that can decrease the light screening phenomena caused by TiO_2 particles, and therefore, facilitate a more efficient utilization of light and avoid the electron-hole recombination [39,52].

The irradiance received on the outer wall of the reactor was measured to get an indirect evaluation of the light screening phenomena. The results are displayed in Figure 2, using a background PFOA (0.24 mmol.L^{-1}) aqueous solution in all cases. The radiation received when using TiO_2 suspensions was significantly lower than through TiO_2-rGO suspensions, for every ultraviolet light range tested and for each catalyst concentration. If we focus on the UV-A range (315-400 nm) and 0.1 g.L^{-1} catalyst dose, where the TiO_2 catalyst can absorb photons to generate the electron/hole pairs, the irradiance

through TiO_2 suspensions was approximately one-tenth of the irradiance received through the TiO_2-rGO solution. These results confirm that TiO_2 particles were promoting the UV light screening and hindered UV-A light penetration through the PFOA solution. While the TiO_2-rGO composite (0.1 $g.L^{-1}$) still reduced the light transmission compared to the absence of catalyst, the suitable photocatalytic properties of the prepared TiO_2-rGO composite overcame the UV light screening, as the achieved PFOA degradation yield (93%) was much higher than the degradation percentage obtained under direct photolysis conditions (58%), as it was reported in Fig. 1.

Some studies have already shown that the combination of TiO_2 with rGO leads to a reduction in the band gap energy to 2.72 eV [48], a feature that would provide the composite TiO_2-rGO with the ability of visible light adsorption, and a more efficient utilization of light than TiO_2 (band gap 3.2 eV). On the other hand, Kamat and co-workers [53,54] have shown that photo-electrons generated by TiO_2 under UV irradiation can be transferred to rGO thanks to the excellent electron conductivity of graphene materials, thus avoiding the electron/hole recombination [43,55]. Therefore, rGO sheets would act as an electron-trap similar to the reported behaviour of the metallic nanoparticles in metal-modified TiO_2 photocatalysts [31,37]. The electron conduction throughout the TiO_2-rGO photocatalyst may further allow higher generation of superoxide and hydroxyl radicals [37,56], which in turn will enhance the oxidation of PFOA molecules.

The structure and morphology of TiO_2-rGO could also have a significant role in the photocatalytic process. It is well known that the spherical-like TiO_2 nanoparticles aggregate to form larger particles [46,56]. Sun et al. [57] demonstrated that UV irradiation of TiO_2 nanoparticles suspended in water accelerated particle aggregation,

that hindered the TiO_2 photocatalytic degradation of Rhodamine B. However, the TiO_2-rGO composite prepared in the present study presented a homogeneous distribution of TiO_2 nanoparticles spread on the platform of a graphene oxide nano-sheet (Fig. S2, supplementary material). This structure may have limited TiO_2 particles agglomeration with the benefit of a more efficient use of the UV light by the composite particles.

Results for experiments performed at different TiO_2-rGO catalyst concentrations are provided in Figure 3. The concentration of the catalyst was first increased from 0.1 $g.L^{-1}$ to 0.5 $g.L^{-1}$, as the latter value is a common dose in TiO_2 photocatalytic experiments, according to the literature survey (Table S1). However, increasing the catalyst dose had the effect of reducing significantly the rate of PFOA removal. Considering that TiO_2 is the major component (95% wt.) of the composite catalyst, the higher concentration of TiO_2 at the highest catalyst dose may have facilitated the UV light screening, as it can be seen in Fig.2. In contrast, the reduction of the catalyst dose to 0.05 $g.L^{-1}$ had a minimal effect on PFOA removal in comparison to 0.1 $g.L^{-1}$ catalyst concentration, in agreement with the similar values of light transmission for 0.05 $g.L^{-1}$ and 0.1 $g.L^{-1}$ TiO_2-rGO concentrations (Fig. 2).

3.2.PFOA Mineralization and intermediate degradation products

Generation of shorter chain PFCAs that were formed as intermediates from PFOA degradation is presented in Fig. 4a, working with a catalyst concentration of 0.1 $g.L^{-1}$. The corresponding fluoride generation for the same experiment is shown in Fig 4b, that also presents the total fluorine in the reactor calculated as the sum of fluoride anions in solution and the fluorine contained as part of the quantified PFCAs. Finally, Fig. 4c presents the reduction of TOC together with the TOC calculated from the organic compounds that were found in the analytical survey. Lines plotted in Figs. 4a and 4c

correspond to simulated vales that were obtained using the model and kinetic parameters that will be described next in this section.

PFOA removal can be described by a first order rate kinetic law. Several studies have reported that PFOA oxidation by hydroxyl radicals proceeds via a stepwise mechanism in which C–C bond cleavage occurs between the carbon chain and the carboxylate group, coupled with fluoride elimination, resulting in the intermediate generation of shorter chain PFCAs [30]. Consistent with this mechanism, in the present work the generation of shorter chain PFCAs was observed. The order of appearance and the concentrations observed in solution support the stepwise degradation mechanism, in which PFOA would have lose one $–CF_2$ group to give PFHpA, and consecutively PFHxA and PFPeA. The next molecule in the degradation pathway would be perfluorobutanoic acid (PFBA) that was detected although at concentrations below the LOD (Limit Of Detection) of the analytical technique. Volatile pefluoropropionic acid (PFPrA) and trifluoroacteic acid (TFA) were not observed in the liquid phase.

TOC was reduced by 62% during the photocatalytic decomposition of PFOA. The difference between the PFOA reduction (93%) and TOC decrease can be ascribed to the presence of intermediate degradation products. It is worth mentioning the good match between the analyzed TOC and the TOC calculated from the quantified concentrations of PFOA, PFHpA, PFHxA, and PFPeA. The coincident trends prove the step-by-step PFOA degradation pathway in which shorter-chain perfluorocarboxylates are the intermediate products.

The gradual increase of fluoride in the aqueous solution demonstrated that the cleavage of the C-F bonds was effective during PFCAs degradation. Total fluorine measurements showed a net loss of fluorine of 20 % after 12 h of photocatalytic treatment. The loss of

fluorine may be attributed to two factors: i) fluoride adsorption on the surface of the TiO_2 fraction of the composite catalysts, which is positively charged in acidic conditions [28,29,58], and ii) the volatilization of the shortest PFCAs obtained as end products of the PFOA degradation chain [33].

In order to verify the possible fluoride incorporation onto the photocatalyst surface, XPS analysis of the TiO_2-rGO particles surface was performed, using both fresh and used samples of the photocatalytic material. The XPS survey spectra and elemental composition for both materials is provided as Fig S6 and Table S2 (supplementary material). As expected, fluorine was only detected on the TiO_2-rGO sample that had been used as catalyst for PFOA photocatalytic degradation. The mass percentual elemental composition of the fresh TiO_2-rGO sample was 13.8/58.1/28.1 as C/O/Ti, while in the used catalyst the elemental composition was 13.1/53.2/26.9/6.8 as C/O/Ti/F.

Fig. 5 shows the section of the high resolution XPS spectrum of used TiO_2-rGO particles, where the F-1s region has been magnified. Three deconvoluted peaks at 684.2 (A), 688.8 (B) and 691.0 eV (C) can be observed: the first peak was related to negatively charged monovalent fluorine (F^-); and the signals around 688-691 eV could be assigned to fluorine bonded to carbon, as it happens in the C-F bonds of PFOA and its perfluorinated degradation intermediates that may have been absorbed on the catalyst surface [28,29]. Moreover, F-1s spectra for TiO_2-rGO composite before use was not detected (Fig. S6). Similar peak distribution and binding energies for raw and used TiO_2-rGO catalysts samples confirmed that the photocatalyst surface remained unchanged after its use in the PFOA photodegradation experiments. Based on the above results, part of the fluoride anions that were released during PFOA abatement were

absorbed onto the TiO_2-rGO photocatalyst, to account for 6.8% of the total mass of the catalyst sample used in the XPS analyses (Table S2). As this adsorption rate did not represent the total fluorine loss, the volatilization of the shortest PFCAs could have also contributed to the 20% of fluorine loss observed in Figure 4b.

Fig. 6 presents the proposed mechanism and pathway of PFOA decomposition in the TiO_2-rGO mediated photocatalysis and the role of rGO in the mechanism. Previous studies considered different possibilities for the initiation of the PFOA molecule oxidation: i) direct reaction of PFOA with the photogenerated holes of the photocatalyst surface [26,29,31,34], ii) indirect reaction with hydroxyl radicals [21,30,36,59,60] or iii) combination of both mechanisms. Thereby, the degradation of PFOA could start from terminal carboxylic end, where the photogenerated hydroxyl radicals can attack the first alkyl C atom adjacent to the -COOH group, leading to the cleavage of C-C bond between the perfluorinated alkyl chain -C_7F_{15} and -COOH by the formation of perfluorinated alkyl radicals, which can then react with water to produce the unstable perfluorinated alcohol $C_7F_{15}OH$ (reactions 1-3). After that, $C_7F_{15}OH$ would eliminate HF to form $C_6F_{13}COF$ (Eq. 4). The active $C_6F_{13}COF$ undergoes hydrolysis in the solution, resulting in the formation of PFHpA with the release of CF_2 unit (Eq. 5).

$$C_7F_{15}COO^- + HO\bullet \rightarrow \bullet C_7F_{15}COO^+ + OH^- \quad (1)$$

$$\bullet C_7F_{15}COO^+ \rightarrow \bullet C_7F_{15} + CO_2 + H^+ \quad (2)$$

$$\bullet C_7F_{15} + H_2O \rightarrow C_7F_{15}OH + H^+ \quad (3)$$

$$C_7F_{15}OH \rightarrow C_6F_{13}COF + F^- + H^+ \quad (4)$$

$$C_6F_{13}COF + H_2O \rightarrow C_6F_{13}COOH + F^- + H^+ \quad (5)$$

On the other hand, other possible initiation of PFOA degradation could be the direct reaction of $C_7F_{15}COO^-$ with the holes. This step would involve the electron transfer

from the dissociated PFOA to the valence band of the photocatalyst, generating the $C_7F_{15}COO\cdot$ radical that subsquentelly would undergo Kolbe descarboxylation, to give perfluoroalkyl radical $C_7F_{15}\cdot$ and CO_2 [34]. The next degradation pathways would be similar to reactions (3) to (5).

Correspondingly, the intermediates will be decomposed stepwisely into shorter-chain PFCAs, and eventually to CO_2 and F^-. Although the reaction mechanism seems to be mostly driven by $HO^\bullet$ radical attack, the formation of the reactive species such as radical superoxide anion ($O_2^{\cdot -}$) may also be associated with the PFOA degradation.

3.3.Kinetic model for PFOA and its degradation products

In a first attempt to quantify the kinetics of PFOA photocatalytic degradation by the TiO_2-rGO composite catalyst, the concentrations of PFOA and intermediate products were fitted to the following first-order rate equation [20,26,28–30,33]:

$$\frac{d[C_n]}{dt} = k_{n+1}\,[C_{n+1}] - k_n\,[C_n] \qquad (6)$$

where *n* is the carbon atoms number in each PFCA molecule, *C* is the concentration in the solution (mmol.L^{-1}), *t* is the time (h), *k* the observed degradation rate constant (h^{-1}) of each PFCA.

Concentration data shown in Figure 4a (0.1 g.L^{-1} TiO_2-rGO) were used for the estimation of kinetic parameters. The obtained values of the apparent kinetic constants can be ordered as $k_{PFPeA} > k_{PFHxA} > k_{PFHpA} > k_{PFOA}$, with values of 2.14, 0.54, 0.27 and 0.163 h^{-1}, respectively. These results point to a clear influence of the length of the perfluoroalkyl chain on the degradation rate. Similarly to our process, Qian et al. [10] reported that the rate constant of PFCAs UV-persulfate decomposition distinctly

increased when the carbon-chain of the PFCAs was shorter.

Eq. (6) and the reported *k* values were used to simulate the concentration of PFCAs, as depicted by the solid lines included in Fig. 4a. Similarly, simulated PFCAs concentrations were employed to calculate TOC evolution, which is also shown as solid line in Fig. 4b. The good agreement between measured and simulated TOC supports the validity of the kinetic constants obtained from the fitting of the experimental results.

4. CONCLUSIONS

This study reports for the first time the effective photocatalytic degradation of perfluorooctanoic acid (PFOA) using a composite catalyst based on TiO_2 and reduced graphene oxide (rGO) successfully synthesized by a hydrothermal method.

The efficient photoactivity of the prepared TiO_2-rGO composite was positively confirmed for PFOA degradation under UV-Visible irradiation. After 12 hours of irradiation, the PFOA removal ratio was as high as 93 ± 7%. using a 0.1 $g.L^{-1}$ concentration of the composite catalyst. The PFOA degradation ratio obtained using TiO_2-rGO was 4-fold higher than the TiO_2-mediated photocatalysis, under the same experimental conditions. It is hypothesized that reduced graphene oxide can efficiently capture the electrons photogenerated by the TiO_2, thus reducing the electron/hole pair recombination, that would promote the PFCAs degradation by means of active radicals or direct oxidation by the photogenerated holes. The progress of shorter-chain perfluorocarboxilyc acids as well as fluoride release elucidated the step-by-step PFOA decomposition mechanism by gradually losing a CF_2 unit in each step, generating CO_2 and F^-. The PFOA mineralization was also demonstrated with the 60% TOC reduction.

Furthermore, the effect of the alkyl chain length on the kinetics of PFCAs was revealed, showing that shorter chain PFCAs degraded faster than their longer chain homologues.

It is concluded that TiO_2-rGO composite catalyst offers an unprecedented effectiveness for the degradation of recalcitrant PFCAs, to become a promising alternative for the photocatalytic degradation of this group of persistent organic pollutants.

APPENDIX A. SUPPLEMENTARY DATA

The supplementary information gathers: a) A survey of literature about PFOA photocatalytic degradation; b) ATR-FTIR spectra, TEM-EDX images and XRD spectra of TiO_2-rGO, GO and TiO_2 materials are provided; c) The experimental setup and the emission spectrum of the medium-pressure mercury lamp; d) XPS results of the TiO_2-rGO surface before and after use in the photocatalytic experiment are also included.

ACKNOWLEDGEMENTS

Financial support from projects CTM2013-44081-R, CTM2015-69845-R and CTM2016-75509-R (MINECO, SPAIN-FEDER 2014–2020) is acknowledged. B. Gomez thanks the FPI scholarship (BES-2014-071045).

REFERENCES

[1] H.J. Lehmler, Synthesis of environmentally relevant fluorinated surfactants - A review, Chemosphere. 58 (2005) 1471–1496.

[2] F. Xiao, M.F. Simcik, T.R. Halbach, J.S. Gulliver, Perfluorooctane sulfonate (PFOS) and perfluorooctanoate (PFOA) in soils and groundwater of a U.S. metropolitan area : Migration and implications for human exposure, Water Res.

72 (2014) 64–74.

[3] S. Fujii, C. Polprasert, S. Tanaka, N.P.H. Lien, Y. Qiu, New POPs in the water environment: Distribution, bioaccumulation and treatment of perfluorinated compounds - A review paper, J. Water Supply Res. Technol. - AQUA. 56 (2007) 313–326.

[4] Secretary-General of the United Nations, The Stockholm convention on persistant organic pollutants, 4 (2009) 1–63. http://chm.pops.int/TheConvention/Overview/TextoftheConvention/tabid/2232/.

[5] USEPA, Drinking Water Health Advisory for Perfluorooctanoic Acid (PFOA), (2016) 1–103. https://www.epa.gov/ground-water-and-drinking-water/drinking-water-health-advisories-pfoa-and-pfos.

[6] M.M. Schultz, C.P. Higgins, C.A. Huset, R.G. Luthy, D.F. Barofsky, J.A. Field, Fluorochemical mass flows in a municipal wastewater treatment facility, Environ. Sci. Technol. 40 (2006) 7350–7357.

[7] I. Fuertes, S. Gómez-Lavín, M.P. Elizalde, A. Urtiaga, Perfluorinated alkyl substances (PFASs) in northern Spain municipal solid waste landfill leachates, Chemosphere. 168 (2017) 399–407.

[8] X. Dauchy, V. Boiteux, C. Bach, A. Colin, J. Hemard, C. Rosin, J.F. Munoz, Mass flows and fate of per- and polyfluoroalkyl substances (PFASs) in the wastewater treatment plant of a fluorochemical manufacturing facility, Sci. Total Environ. 576 (2017) 549–558.

[9] R. Qu, J. Liu, C. Li, L. Wang, Z. Wang, J. Wu, Experimental and theoretical insights into the photochemical decomposition of environmentally persistent perfluorocarboxylic acids, Water Res. 104 (2016) 34–43.

[10] Y. Qian, X. Guo, Y. Zhang, Y. Peng, P. Sun, C.H. Huang, J. Niu, X. Zhou, J.C. Crittenden, Perfluorooctanoic Acid Degradation Using UV-Persulfate Process: Modeling of the Degradation and Chlorate Formation, Environ. Sci. Technol. 50 (2016) 772–781.

[11] Y. Qu, C. Zhang, F. Li, J. Chen, Q. Zhou, Photo-reductive defluorination of perfluorooctanoic acid in water, Water Res. 44 (2010) 2939–2947.

[12] C.R. Estrellan, C. Salim, H. Hinode, Photocatalytic decomposition of perfluorooctanoic acid by iron and niobium co-doped titanium dioxide, J. Hazard. Mater. 179 (2010) 79–83.

[13] Á. Soriano, D. Gorri, A. Urtiaga, Efficient treatment of perfluorohexanoic acid by nanofiltration followed by electrochemical degradation of the NF concentrate, Water Res. 112 (2017) 147–156.

[14] B. Gomez-Ruiz, S. Gómez-Lavín, N. Diban, V. Boiteux, A. Colin, X. Dauchy, A. Urtiaga, Efficient electrochemical degradation of poly- and perfluoroalkyl substances (PFASs) from the effluents of an industrial wastewater treatment plant, Chem. Eng. J. 322 (2017) 196–204.

[15] C.E. Schaefer, C. Andaya, A. Burant, C.W. Condee, A. Urtiaga, T.J. Strathmann, C.P. Higgins, Electrochemical treatment of perfluorooctanoic acid and perfluorooctane sulfonate: insights into mechanisms and application to groundwater treatment, Chem. Eng. J. (2017).

[16] A. Urtiaga, C. Fernández-González, S. Gómez-Lavín, I. Ortiz, Kinetics of the electrochemical mineralization of perfluorooctanoic acid on ultrananocrystalline boron doped conductive diamond electrodes, Chemosphere. 129 (2015) 20–26.

[17] H. Hori, A. Yamamoto, E. Hayakawa, S. Taniyasu, N. Yamashita, S. Kutsuna, H. Kiatagawa, R. Arakawa, Efficient decomposition of environmentally persistent perfluorocarboxylic acids by use of persulfate as a photochemical oxidant, Environ. Sci. Technol. 39 (2005) 2383–2388.

[18] C.D. Vecitis, H. Park, J. Cheng, B.T. Mader, M.R. Hoffmann, Kinetics and Mechanism of the Sonolytic Conversion of the Aqueous Perfluorinated Surfactants, Perfiuorooctanoate (PFOA), and Perfluorooctane Sulfonate (PFOS) into Inorganic Products, J. Phys. Chem. A. 112 (2008) 4261–4270.

[19] H. Hori, E. Hayakawa, H. Einaga, S. Kutsuna, K. Koike, T. Ibusuki, H. Kiatagawa, R. Arakawa, Decomposition of environmentally persistent

perfluorooctanoic acid in water by photochemical approaches, Environ. Sci. Technol. 38 (2004) 6118–6124.

[20] M.H. Cao, B.B. Wang, H.S. Yu, L.L. Wang, S.H. Yuan, J. Chen, Photochemical decomposition of perfluorooctanoic acid in aqueous periodate with VUV and UV light irradiation, J. Hazard. Mater. 179 (2010) 1143–1146.

[21] Y.C. Chen, S.L. Lo, J. Kuo, Effects of titanate nanotubes synthesized by a microwave hydrothermal method on photocatalytic decomposition of perfluorooctanoic acid, Water Res. 45 (2011) 4131–4140.

[22] M. Pelaez, N.T. Nolan, S.C. Pillai, M.K. Seery, P. Falaras, A.G. Kontos, P.S.M. Dunlop, J.W.J. Hamilton, J.A. Byrne, K. O'Shea, M.H. Entezari, D.D. Dionysiou, A review on the visible light active titanium dioxide photocatalysts for environmental applications, Appl. Catal. B Environ. 125 (2012) 331–349.

[23] S. Dominguez, P. Ribao, M.J. Rivero, I. Ortiz, Influence of radiation and TiO_2 concentration on the hydroxyl radicals generation in a photocatalytic LED reactor. Application to dodecylbenzenesulfonate degradation, Appl. Catal. B Environ. 178 (2014) 165–169.

[24] M. Sanchez, M.J. Rivero, I. Ortiz, Kinetics of dodecylbenzenesulphonate mineralisation by TiO_2 photocatalysis, Appl. Catal. B Environ. 101 (2011) 515–521.

[25] R. Dillert, D. Bahnemann, H. Hidaka, Light-induced degradation of perfluorocarboxylic acids in the presence of titanium dioxide, Chemosphere. 67 (2007) 785–792.

[26] S.C. Panchangam, A.Y.C. Lin, K.L. Shaik, C.F. Lin, Decomposition of perfluorocarboxylic acids (PFCAs) by heterogeneous photocatalysis in acidic aqueous medium, Chemosphere. 77 (2009) 242–248.

[27] Y. Wang, P. Zhang, Photocatalytic decomposition of perfluorooctanoic acid (PFOA) by TiO_2 in the presence of oxalic acid, J. Hazard. Mater. 192 (2011) 1869–1875.

[28] M. Sansotera, F. Persico, C. Pirola, W. Navarrini, A. Di Michele, C.L. Bianchi, Decomposition of perfluorooctanoic acid photocatalyzed by titanium dioxide: Chemical modification of the catalyst surface induced by fluoride ions, Appl. Catal. B Environ. 148–149 (2014) 29–35.

[29] S. Gatto, M. Sansotera, F. Persico, M. Gola, C. Pirola, W. Panzeri, W. Navarrini, C.L. Bianchi, Surface fluorination on TiO_2 catalyst induced by photodegradation of perfluorooctanoic acid, Catal. Today. 241 (2015) 8–14.

[30] M.J. Chen, S.L. Lo, Y.C. Lee, C.C. Huang, Photocatalytic decomposition of perfluorooctanoic acid by transition-metal modified titanium dioxide, J. Hazard. Mater. 288 (2015) 168–175.

[31] M. Li, Z. Yu, Q. Liu, L. Sun, W. Huang, Photocatalytic decomposition of perfluorooctanoic acid by noble metallic nanoparticles modified TiO_2, Chem. Eng. J. 286 (2016) 232–238.

[32] C. Song, P. Chen, C. Wang, L. Zhu, Photodegradation of perfluorooctanoic acid by synthesized TiO_2-MWCNT composites under 365nm UV irradiation, Chemosphere. 86 (2012) 853–859.

[33] X. Li, P. Zhang, L. Jin, T. Shao, Z. Li, J. Cao, Efficient photocatalytic decomposition of perfluorooctanoic acid by indium oxide and its mechanism., Environ. Sci. Technol. 46 (2012) 5528–34.

[34] M. Sansotera, F. Persico, V. Rizzi, W. Panzeri, C. Pirola, C.L. Bianchi, A. Mele, W. Navarrini, The effect of oxygen in the photocatalytic oxidation pathways of perfluorooctanoic acid, J. Fluor. Chem. 179 (2015) 159–168.

[35] S.C. Panchangam, A.Y.C. Lin, J.H. Tsai, C.F. Lin, Sonication-assisted photocatalytic decomposition of perfluorooctanoic acid, Chemosphere. 75 (2009) 654–660.

[36] M.J. Chen, S.L. Lo, Y.C. Lee, J. Kuo, C.H. Wu, Decomposition of perfluorooctanoic acid by ultraviolet light irradiation with Pb-modified titanium dioxide, J. Hazard. Mater. 303 (2016) 111–118.

[37] P. Ribao, M.J. Rivero, I. Ortiz, TiO_2 structures doped with noble metals and/or graphene oxide to improve the photocatalytic degradation of dichloroacetic acid, Environ. Sci. Pollut. Res. (2016) 1–10.

[38] D. Liang, C. Cui, H. Hub, Y. Wang, S. Xu, B. Ying, P. Li, B. Lu, H. Shen, One-step hydrothermal synthesis of anatase TiO_2/reduced graphene oxide nanocomposites with enhanced photocatalytic activity, J. Alloys Compd. 582 (2014) 236–240.

[39] H. Zhang, X. Lv, Y. Li, Y. Wang, J. Li, P25-graphene composite as a high performance photocatalyst, ACS Nano. 4 (2009) 380–386.

[40] H. Adamu, P. Dubey, J.A. Anderson, Probing the role of thermally reduced graphene oxide in enhancing performance of TiO_2 in photocatalytic phenol removal from aqueous environments, Chem. Eng. J. 284 (2016) 380–388.

[41] Y. Liang, H. Wang, H.S. Casalongue, Z. Chen, H. Dai, TiO_2 Nanocrystals grown on graphene as advanced photocatalytic hybrid materials, Nano Res. 3 (2010) 701–705.

[42] H. Zhao, J. Gao, G. Zhao, J. Fan, Y. Wang, Y. Wang, Fabrication of novel SnO_2-Sb/carbon aerogel electrode for ultrasonic electrochemical oxidation of perfluorooctanoate with high catalytic efficiency, Appl. Catal. B Environ. 136–137 (2013) 278– 286.

[43] P. Wang, J. Wang, X. Wang, H. Yu, J. Yu, M. Lei, Y. Wang, One-step synthesis of easy-recycling TiO_2-rGO nanocomposite photocatalysts with enhanced photocatalytic activity, Appl. Catal. B Environ. 132–133 (2013) 452–459.

[44] R.K. Nainani, P. Thakur, Facile synthesis of TiO_2-RGO composite with enhanced performance for the photocatalytic mineralization of organic pollutants, Water Sci. Technol. 73 (2016) 1927–1936.

[45] B. Neppolian, A. Bruno, C.L. Bianchi, M. Ashokkumar, Graphene oxide based Pt-TiO_2 photocatalyst: Ultrasound assisted synthesis, characterization and catalytic efficiency, Ultrason. Sonochem. 19 (2012) 9–15.

[46] L.M. Pastrana-Martínez, S. Morales-Torres, V. Likodimos, J.L. Figueiredo, J.L. Faria, P. Falaras, A.M.T. Silva, Advanced nanostructured photocatalysts based on reduced graphene oxide-TiO_2 composites for degradation of diphenhydramine pharmaceutical and methyl orange dye, Appl. Catal. B Environ. 123–124 (2012) 241–256.

[47] W.S. Hummers, R.E. Offeman, Preparation of Graphitic Oxide, J. Am. Chem. Soc. 80 (1958) 1339–1339.

[48] J. Li, S.L. Zhou, G.B. Hong, C.T. Chang, Hydrothermal preparation of P25-graphene composite with enhanced adsorption and photocatalytic degradation of dyes, Chem. Eng. J. 219 (2013) 486–491.

[49] J. Chen, P. Zhang, J. Liu, Photodegradation of perfluorooctanoic acid by 185 nm vacuum ultraviolet light, J. Environ. Sci. 19 (2007) 387–390.

[50] R.R. Giri, H. Ozaki, T. Morigaki, S. Taniguchi, R. Takanami, UV photolysis of perfluorooctanoic acid (PFOA) in dilute aqueous solution, Water Sci. Technol. 63 (2011) 276–282.

[51] N.A. Ab Aziz, P. Palaniandy, H.A. Aziz, I. Dahlan, Review of the mechanism and operational factors influencing the degradation process of contaminants in heterogenous photocatalysis, J. Chem. Res. 40 (2016) 704–712.

[52] H.A. Becerril, J. Mao, Z. Liu, R.M. Stoltenberg, Z. Bao, Y. Chen, Evaluation of Solution-Processed Reduced Graphene Oxide Films as Transparent Conductors, ACS Nano. 2 (2008) 463–470.

[53] G. Williams, B. Seger, P. V. Kamat, TiO_2-graphene nanocomposites. UV-assisted photocatalytic reduction of graphene oxide, ACS Nano. 2 (2008) 1487–1491.

[54] I. V. Lightcap, T.H. Kosel, P. V. Kamat, Anchoring semiconductor and metal nanoparticles on a two-dimensional catalyst mat. storing and shuttling electrons with reduced graphene oxide, Nano Lett. 10 (2010) 577–583.

[55] H. Mahmood, A. Habib, M. Mujahid, M. Tanveer, S. Javed, A. Jamil, Band gap

reduction of titania thin films using graphene nanosheets, Mater. Sci. Semicond. Process. 24 (2014) 193–199.

[56] M.J. Sampaio, C.G. Silva, A.M.T. Silva, L.M. Pastrana-Martínez, C. Han, S. Morales-Torres, J.L. Figueiredo, D.D. Dionysiou, J.L. Faria, Carbon-based TiO_2 materials for the degradation of Microcystin-LA, Appl. Catal. B Environ. 170–171 (2015) 74–82.

[57] J. Sun, L.-H. Guo, H. Zhang, L. Zhao, UV Irradiation Induced Transformation of TiO_2 Nanoparticles in Water: Aggregation and Photoreactivity, Environ. Sci. Technol. 48 (2014) 11962–11968.

[58] M.S. Vohra, S. Kim, W. Choi, Effects of surface fluorination of TiO_2 on the photocatalytic degradation of tetramethylammonium, J. Photochem. Photobiol. A Chem. 160 (2003) 55–60.

[59] C. Song, P. Chen, C. Wang, L. Zhu, Photodegradation of perfluorooctanoic acid by synthesized TiO_2-MWCNT composites under 365nm UV irradiation, Chemosphere. 86 (2012) 853–859.

[60] H. Tang, Q. Xiang, M. Lei, J. Yan, L. Zhu, J. Zou, Efficient degradation of perfluorooctanoic acid by UV – Fenton process, Chem. Eng. J. 184 (2012) 156–162.

Figure captions

Fig. 1. Evolution of PFOA concentration (mmol.L^{-1}) with irradiation time by photolysis and photocatalysis using TiO_2 and TiO_2-rGO; photocatalyst loading: 0.1 g.L^{-1}.

Fig. 2. Irradiance measurements (W.m^{-2}) on the outer wall of the reactor using TiO_2 (0.05, 0.1 and 0.5 g.L^{-1}, red bars) and TiO_2-rGO suspensions (0.05, 0.1 and 0.5 g.L^{-1}, green bars) in a PFOA (0.24 mmol.L^{-1}) aqueous solution, in the regions: UV-A (315-400 nm), UV-B (280-315 nm) and UV-C (110-280 nm).

Fig. 3. Influence of the TiO_2-rGO loading on the PFOA concentration (mmol.L^{-1}) with the irradiance time. TiO_2-rGO concentrations were 0.05, 0.1 and 0.5 g.L^{-1}.

Fig. 4. Evolution of (A) PFOA, PFHpA, PFHxA and PFPeA (mmol.L^{-1}), and their simulated concentrations using the pseudo-first order estimated kinetic parameters (solid line); (B) fluoride (mmol.L^{-1}) in solution and calculated total fluorine (%), and (C) measured TOC/TOC_0, calculated TOC/TOC_0 from the analyzed PFCAs, and simulated TOC/TOC_0 using the simulated PFCAs concentrations. Experimental data obtained using 0.1 g.L^{-1} of TiO_2-rGO. TOC_0 was the initial value in each experiment.

Fig 5. XPS spectrum in the F-1s region of TiO_2-rGO surface after PFOA photocatalytic degradation. A peak is attributed to inorganic fluorinated species. B and C peaks are assigned to organic fluorinated compounds.

Fig. 6. Photocatalytic pathways of PFOA decomposition using the TiO_2-rGO catalyst.

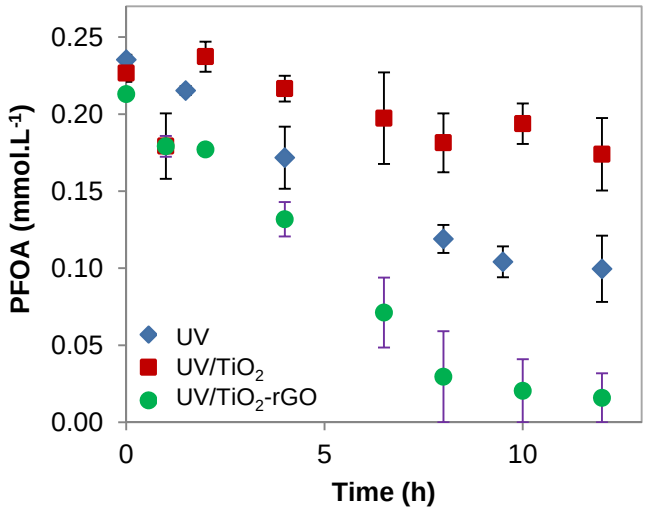

Fig. 1.

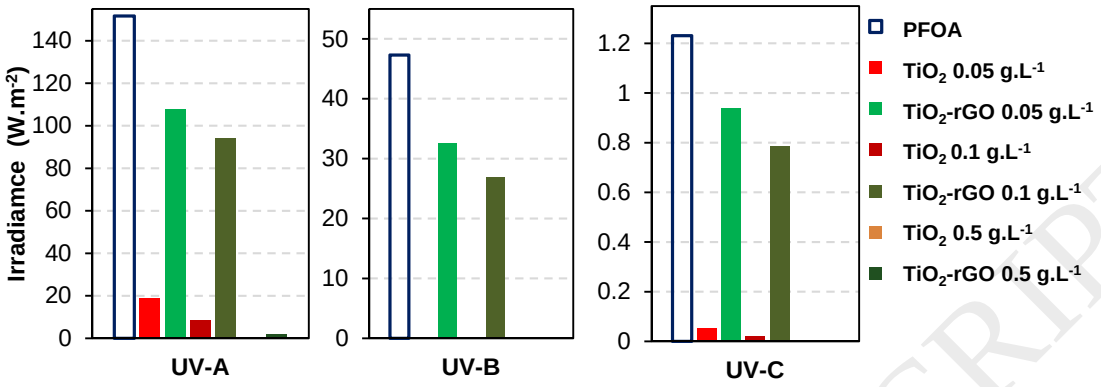

Fig. 2.

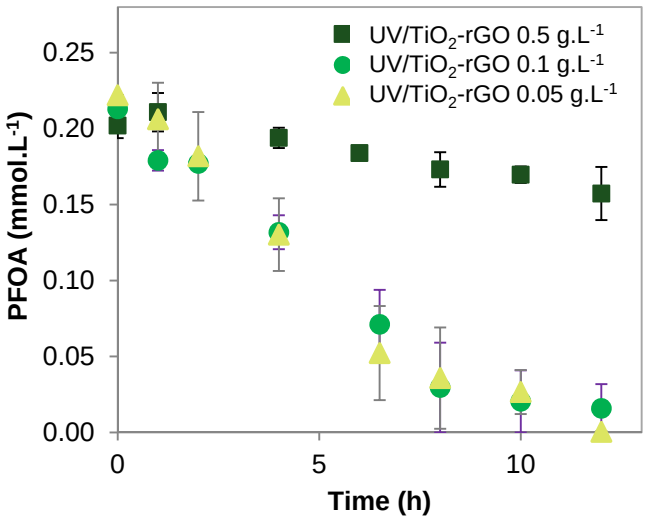

Fig. 3.

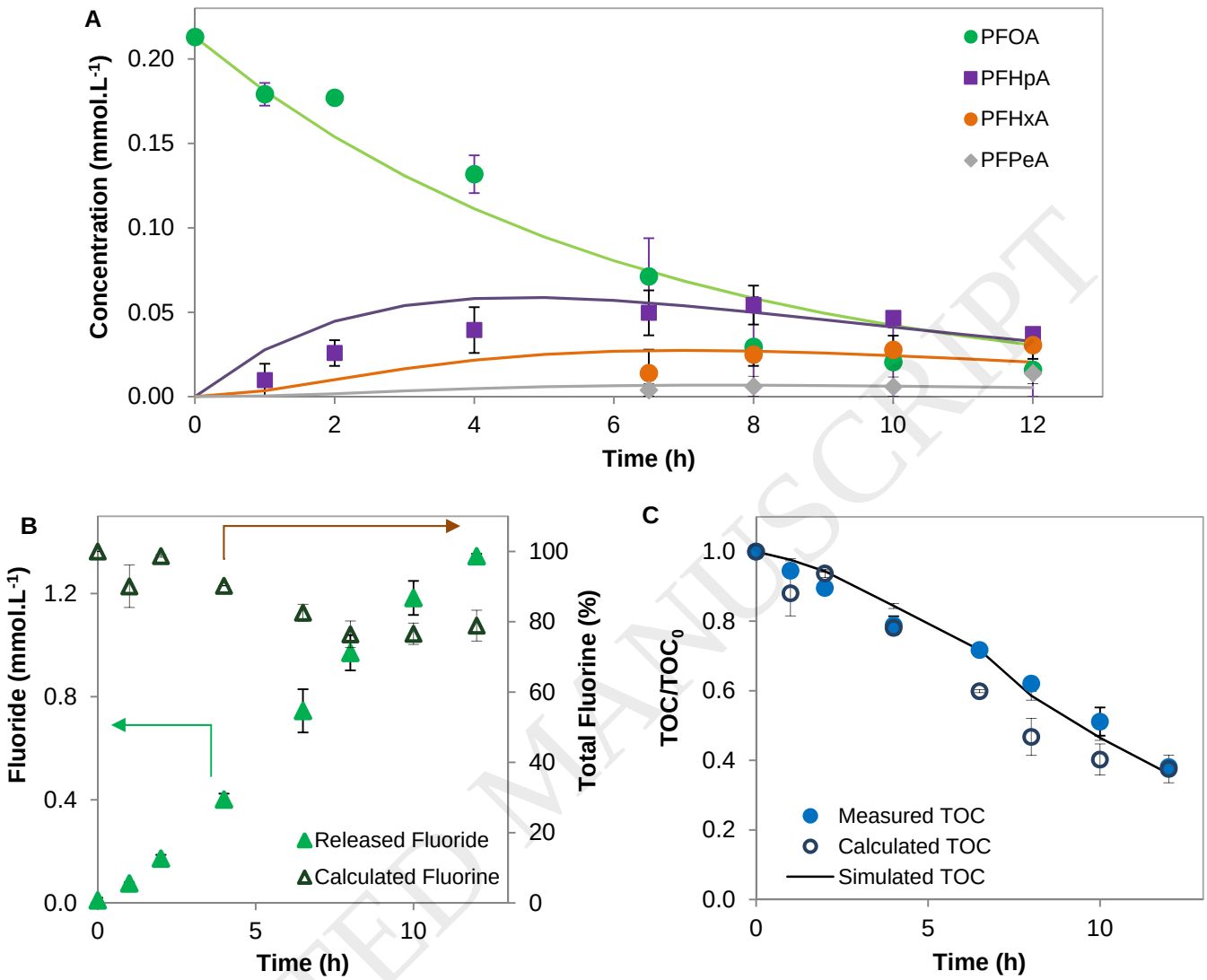

Fig. 4.

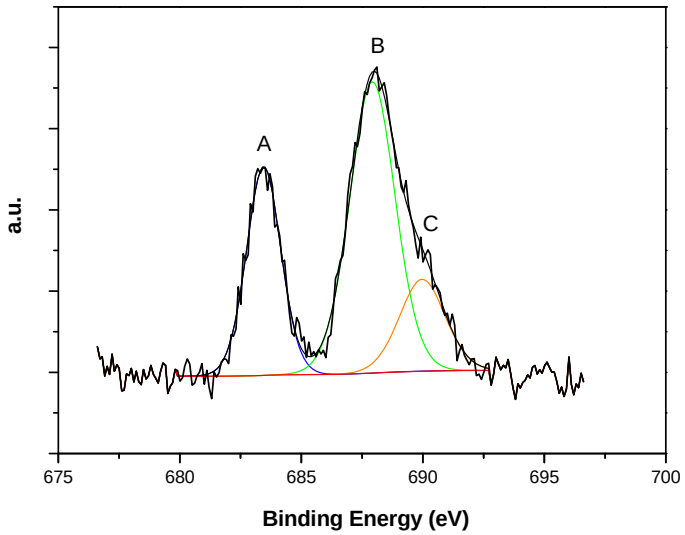

Fig 5.

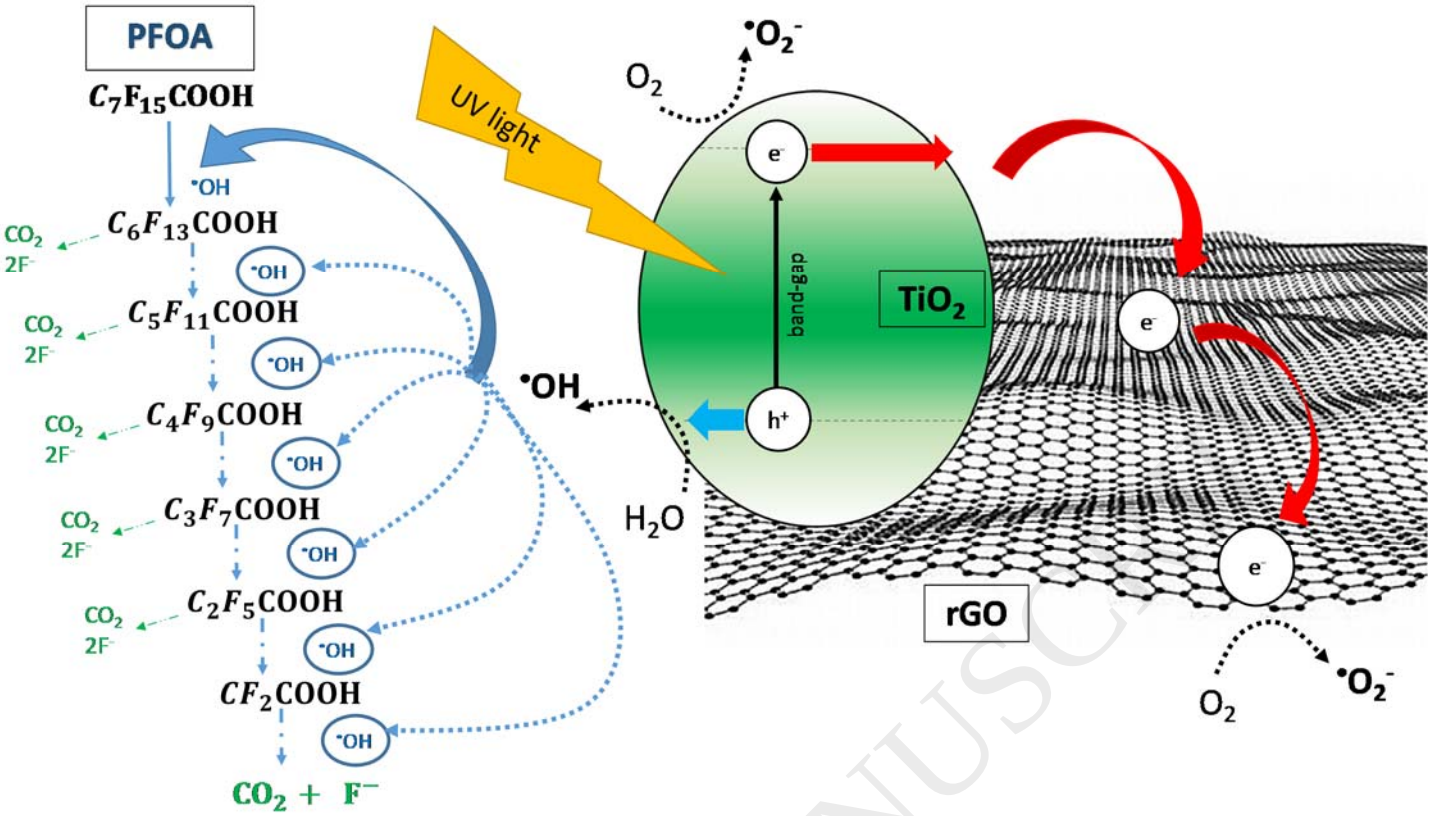

Fig. 6